Energy Conversion and Management: X 25 (2025) 100848

Contents lists available at ScienceDirect

Energy Conversion and Management: X

journal homepage: www.sciencedirect.com/journal/energy-conversion-and-management-x

Experimental investigation of the effect of intermittent operation on membranes in wind-powered SWRO plants, focusing on frequent start-stop scenarios

José A. Carta [a], Pedro Cabrera [a,*], Noemi Melián-Martel [b], Sigrid Arenas-Urrea [c]

[a] Department of Mechanical Engineering, University of Las Palmas de Gran Canaria, Campus de Tafira S/n, 35017 Las Palmas de Gran Canaria, Spain
[b] Department of Process Engineering, University of Las Palmas de Gran Canaria, Campus de Tafira s/n, 35017 Las Palmas de Gran Canaria, Spain
[c] Water Department, Canary Islands Institute of Technology (ITC), Playa de Pozo Izquierdo s/n, 35119 Santa Lucía-Las Palmas, Spain

ARTICLE INFO

Keywords:
Intermittent operation
Off-grid wind-driven desalination
Pretreatment
Normalized parameters
Membrane autopsy

ABSTRACT

Given the temporal variability of wind, the intermittent operation of off-grid wind-powered seawater reverse osmosis (SWRO) desalination plants has been proposed. However, it has also been suggested that intermittency may damage plant membranes. This paper presents the results and analysis of testing a 100 m^3/day rated capacity SWRO plant (two pressure vessels, 1:1 arrangement with 5 and 2 membrane elements [Hydranautics 6-SWC4-LD] per pressure vessel). For over 4 months (totaling 3,136 h), the SWRO plant was operated intermittently—1 h on and 1 h off—24 h each day, resulting in 1,568 start-stop cycles. The evolution of various parameters was analyzed using machine learning techniques, hypothesis testing, and effect size analysis. At the end of the test period, membrane autopsies were conducted on the first and last membranes of the system.

The results show that cumulative intermittent operating hours significantly influenced the normalized permeate flow (NPF increased slightly by 0.0065 m^3/h), normalized salt rejection (NSR increased by 0.12 %), normalized salt permeate concentration (NSPC decreased by 4.5 mg/L), and normalized pressure differential (NPD showed no significant change). Statistical analysis indicated that the statistically significant differences between the means of these normalized parameters at the start and end of the test are primarily the result of changes in operating parameters—such as feed water temperature (decreased by 1.2 °C) and conductivity (decreased by 527 mg/L)—rather than membrane degradation. According to the autopsies, only slight fouling was detected and no telescoping effect was observed. The integrity tests were negative, except for the methylene blue test, which detected some abrasion marks on the polyamide layer due to displacement of the feed channel spacers.

These results provide useful information about the behavior of wind-powered SWRO systems with a high number of starts and stops, suggesting that frequent intermittent operation does not significantly damage SWRO membranes over the tested period.

Introduction

According to Alawad *et al.* [1], different problems are being generated by the dramatic increase in the demand for desalinated water, including that of a reater need for fossil fuel consumption for power production. Thiel *et al.* [2] estimated that the desalination plants currently in operation around the world emit each year around 120 million tons of CO_2. If low-carbon options are not implemented this amount could rise to as much as 218 million tons by 2040[3]. In this context, Aboelmaaref *et al.* [4] highlighted that reducing the negative effect of global warming requires the urgent implementation of renewable energies (REs) in desalination processes.

According to Ghaffour *et al.* [5], only about 1 % of total desalinated water is currently based on RE-sourced energy. However, Ghazi *et al.* [6] have reported how even countries with their own fossil fuel energy resources are planning to incorporate REs in this regard in order to promote a sustainable future for their citizens and at the same time to meet the requirements established to combat climate change [7].

Proposals have been made for the deployment of different types of RE to power desalination technologies [6,8–10]. According to Yilmaz [10], depending on the geographical location, more efficient systems

* Corresponding author.
E-mail address: pedro.cabrerasantana@ulpgc.es (P. Cabrera).

https://doi.org/10.1016/j.ecmx.2024.100848
Received 11 July 2024; Received in revised form 17 December 2024; Accepted 19 December 2024
Available online 27 December 2024

Nomenclature

∧	Symbol assigned to a variable (feature) estimated by an RF model
π_{fb}	Feed-brine osmotic pressure, bar
π_P	Permeate osmotic pressure, bar
$\Delta P_{fb}/2=(P_f - P_b)/2$	One half device pressure drop, bar
$\Delta_p = P_{sf} - P_{hpp}$	Filters pressure drop, bar
'*a*' and '*r*'	Refer to the actual and referenced measurement values
ASTM	American Society for Testing and Materials
BWRO	Brackish water reverse osmosis
C_f	Feed concentration, mg/L
C_{fb}	Feed-brine concentration, mg/L
C_p	Permeate concentration, mg/L
DI	Deionized water
MAE	Mean absolute error, in the same units as the parameters it compares
ML	Machine learning
NPD	Normalized pressure differential, bar
NPF	Normalized permeate flow, m^3/h
NSPC	Normalized salt permeate concentration, mg/L
NSR	Normalized salt rejection, %
OB	Osmotic backwash
P_b	Brine pressure, bar
Pf	Feed pressure, bar
P_{hpp}	Pressure at the inlet of the high pressure pump, bar
Pp	Permeate pressure, bar
P_{sf}	Pressure at the inlet of the sand filter, bar
PV	Photovoltaics
Q_f	Feed flow, m^3/h
R^2	Adjusted coefficient of determination, %
RE	Renewable energy
RF	Random forest
RMSE	Root mean square error, in the same units as the parameters it compares
RO	Reverse osmosis
SP	Percent salt passage, %
STCF	Salt transport temperature correction factor
SWRO	Sea water reverse osmosis
TCF	Temperature correction factor
WF	Wind farm
WT	Wind turbine
Y	Conversion

can be achieved by combining wind, solar, hydropower and other REs. However, according to Cherif *et al.* [11], compared to other RE sources, solar and wind energy tend to have much greater availability in geographic regions with water scarcity issues and are presently considered to be the most suitable options to power desalination process. Furthermore, according to Abdelkareem *et al.* [12], these are the two RE sources most commonly used for desalination (with hybrid RE sources used in just 10 % of cases). Of the desalination technologies that can be employed, reverse osmosis (RO) predominates [12,13].

Strategies employing RE that have been used to date to electrically power large-scale desalination plants have mainly been based on the use of wind energy and connection of the wind farms (WFs) and desalination plants to the main grid [14]. Such installations basically employ two strategies for wind and conventional energy management when it comes to powering the desalination plants [14–16]. With both strategies, the desalination plants generally work in continuous mode and without frequent interruptions. However, for various reasons, a significant number of proposals have been made for employment of the off-grid strategy for RE-driven desalination systems, especially small- and medium-scale types [14,16]. As pointed out by Alawad *et al.* [1], one of the most challenging problems when using REs is their intermittent behaviour. In this context, and with respect to the off-grid strategy for RE-driven desalination systems, various proposals have been made to deploy massive energy storage systems [16–18] or hybrid energy systems [16,18–20], which would allow RO plants to work under constant operating conditions despite the temporal variability of the RE. In this case, the frequency of the starts/stops of an RO plant is conditioned by the capacity of the energy storage system used [17,21].

According to Alawad *et al.* [1], no currently available energy storage device is ideal. In this context, it should be noted that numerous proposals have been made to dispense with the use of backup devices in seawater RO (SWRO) plants and instead have the plants adapt their operation to the temporal variability of the RE-generated energy [22–26]. Cabrera *et al.*[27], provide detailed information about the numerous lessons that have been learnt from the many experiments and projects that have been developed in the Canary Archipelago since 1984 in the field of wind energy-desalination. The results obtained in tests undertaken in the islands with SWRO plants working under variable pressure and flow conditions showed that they can operate satisfactorily with high recovery rates (up to 50 %) without problems arising. However, the drawbacks that have been attributed to RE-driven desalination systems operating intermittently include, importantly, potential RO membrane damage [28].

1.1. Literature review on the effects of the intermittent operation of RO plants

From the ealry 1970 s, when research on desalination with RES began, one of the main technical challenges has been the stand-alone operation of the system due to their temporal variability [29,30]. In this context, in 1981 Petersen *et al.* [31] and in 1987 McBride *et al.* [32] provided information about the operation of an RO unit powered by a wind turbine (WT) on the island of Suderoog, the initial configuration of which had been described in 1979 by Petersen *et al.* [33]. According to McBride *et al.* [32], after a series of modifications, the system was in operation from August 1982 to July 1983 and the RO plant showed no unfavourable effects as a result of the stop/start cycles. In the same paper [32], the authors described the performance of a WT-powered RO plant on the island of Planier, which had been presented in 1979 by Maurel [34] and in 1981 by Libert and Maurel [35]. According to McBride *et al.* [32], the main problem was the frequency of the starts/stops, especially when the wind speed was close to the start-up speed of the WT.

Carta *et al.*[23] provided an operational analysis of a fully autonomous wind-powered desalination system (called SDAWES) with a rated capacity of 200 m^3/d (8 SWRO modules with 25 m^3/d capacity). Among other tasks, the automated operating strategy controlled the number of SWRO modules that had to be connected or disconnected at any given time to enable, working under practically constant operating conditions, adaptation to the variable wind energy supply (Fig. 1). According to the authors [23], in the years in which the prototype was tested, no significant variation was found in the level of quality or average volume of the product water, nor any physical deterioration to the main components of the system as a result of the starts/stops required because of the variations in the wind energy supply. To reduce the start/stop frequency of SWRO modules when wind speeds are low, the authors recommended programming into the control software the appropriate wind speed threshold for system start-up, which would vary according to the wind regime at the site in question and the characteristics of the system design. Optimization of the moment of start-up initiation should be

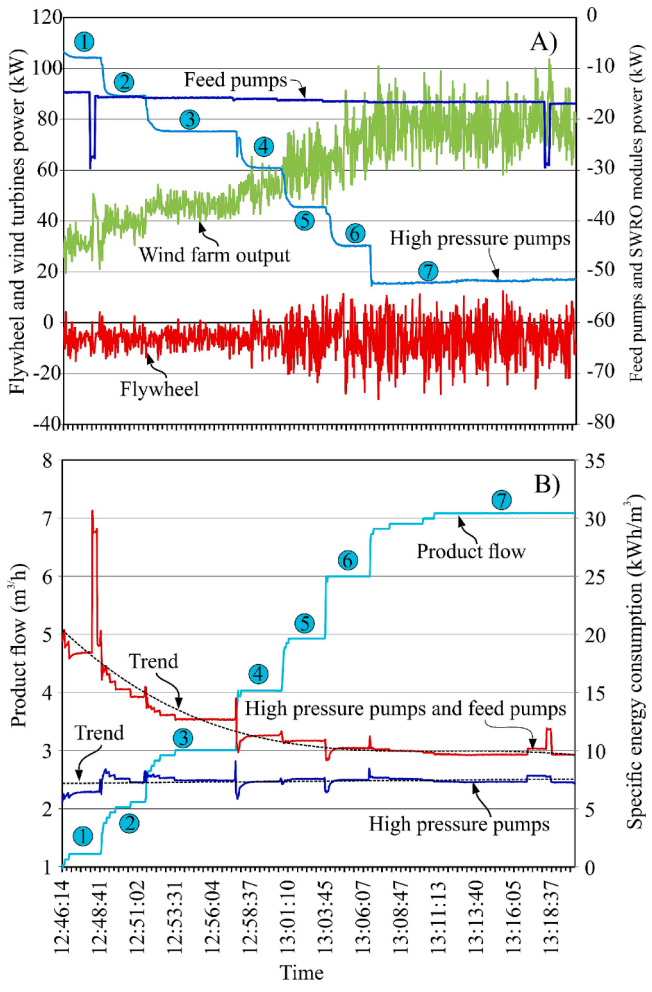

Fig. 1. SDAWES project: Sequential connection process of seven SWRO modules (13/10/2000, from 12:46:14 to 13:20:09. A) Power, B) Product flow and specific energy consumption.

based on wind speed prediction models. According to the authors[23], several more years of tests would be required to establish definitive conclusions about the effects of intermittent operation on the useful life of the membranes. In this context, it should be noted that, according to Byrne [36] and with respect to membrane replacement just 3 years of useful life has become a common assumption (with a probable relation to the duration of the manufacturer's guarantee). However, according to Voutchkov [37], the useful life of RO membranes is typically between 5 and 7 years, and, in the case of high-quality source seawater, it may be as much as 10 years.

According to Jiang *et al.* [38], one of the factors affecting bacteria attachment to a membrane surface is the operating conditions. In this context, in 2016 Lai *et al.* [28] aimed to describe, based on references, the effects of wind intermittence on RO desalination. However, their work focused fundamentally on the effects on membranes produced by flow and pressure fluctuations and to a lesser extent by intermittent operation of the plant. In other words, their study was not centred on the potential effects that frequent RO plant starts/stops might have on the membranes and, in addition, the references they used were in relation to works carried out on very small laboratory prototypes tested over a very small time period.

Park *et al.* [39], to determine the effect of intermittent operation, tested a Filmtec BW30-4040 brackish water RO (BWRO) membrane with feedwaters of 2,750 mg/L and 5,500 mg/L NaCl with interruptions of 0.5 to 3 min. To determine the effect of intermittent operation on the quality and quantity of the permeate, they performed tests lasting one hour with six start/stop cycles and averaged the efficiency parameters for this time period. According to the authors [39], the longest periods without energy (1 to 3 min) had no significant effect on mean water quality.

Freire-Gormaly and Bilton [40,41] performed an experimental test of a BWRO plant at laboratory scale. The intermittent operation test was carried out for 3 days, with 8 h of operation and 16 h of shutdown each day. The aim was to evaluate the effect of intermittent operation compared to continuous operation for a lab-mixed brackish water. According to the authors [41], the results showed that intermittent operation did not cause a significant decline in membrane permeability compared to continuous operation. In the same study [41] they evaluated the effects on membrane permeability of intermittent operation, antiscalant pre-treatment and membrane rinsing prior to shutdown over a longer operating period (3–6 days). The analysis they conducted, comparing intermittent and continuous operation, the use of antiscalant and membrane rinsing with permeate water, showed that minimizing the decline in membrane permeability depended most on membrane rinsing with permeate water.

Sarker and Bilton [42], in a heavy mineral scaling ($CaSO_4$) scenario, undertook continuous (24 h) and intermittent (8 h/d x 3 d) tests with a plate-and-frame RO module that they expressly designed and manufactured to understand the impacts of intermittency typically seen in small-scale plants. They detected no negative effect of periodic shutdowns on flux decline, which is contrary to the perception that intermittent operation decreases membrane permeability.

Kim *et al.*[43] investigated the biofouling phenomenon in a pilot-scale BWRO plant under different artificial saline groundwater conditions (oxic and anoxic) and operating modes (continuous and intermittent). To simulate the intermittent mode, the BWRO plant was in operation for 5 h and stopped for 19 h each day for 7 days. In continuous mode, the BWRO system was in operation for 35 h. According to the authors [43], the results suggest that intermittent operation and chemical cleaning could be effective strategies to mitigate biofouling in BWRO plants treating saline waters.

Lee *et al.* [44] investigated, at laboratory scale, the fouling of pressurized RO membranes (RE4040-BE, Toray) under intermittent operation using an approach based on optical coherence tomography. The RO tests were performed in continuous and intermittent mode. To simulate the intermittent operating cycles for RE-powered RO systems, 8 h of operation and 16 h of shutdown were repeated each day for five days. In the case of intermittent operation, two strategies were evaluated. In one, the membrane was stored in the feedwater during the shutdown, and in the other the membrane was rinsed with distilled water for 5 min and then stored in distilled water for the rest of the shutdown period. According to the authors [44], the analysis undertaken showed that foulant thickness was significantly reduced with the intermittent operation.

Yang *et al.* [45] examined the effect of intermittent operation on membrane fouling using a laboratory scale desalination plant, The RO plant comprised 4 flat membrane modules. The feed solutions were prepared using NaCl, $CaSO_4$ and colloidal silica. They used NaCl to prepare the synthetic seawater and set its concentration at 32,000 mg/L. Feed flow and pressure were constant during the RO operation. Four intermittent operation modes were compared: feed solution recirculation, membrane storage in the feed solution, deionized water (DI) recirculation, and membrane storage in DI water. They considered minimum (4 h) and maximum (14 h) operating times. Three stops of 3 h duration were made during the tests. The results showed that intermittent operation reduced fouling. However, the extent of fouling mitigation differed depending on the feed conditions, foulant type and the membrane lay-up (storage) method employed.

Ruiz-García and Nuez [46] analysed the operating data over 14 years (~9h d^{-1}), without membrane replacement, of an intermittently operated BWRO desalination plant designed to desalinate underground waters for crop irrigation (mainly tomatoes). They concluded that daily shutdowns and start-ups did not cause the plant additional problems,

indicating that the intermittent operation of desalination plants is feasible over the long term. In this context, it should be noted that intermittent operation with overnight shutdowns is usually associated with desalination plants powered with solar photovoltaic (PV) energy. However, considerably longer shutdown periods have been associated with wind-powered desalination plants [19,20].

Cai *et al.* [47], used a bench-scale nanofiltration-RO (flat sheet membranes) crossflow system powered by a solar array simulator to test the effect of intermittency caused by periodic irradiance fluctuations on membrane performance. Synthetic brackish feedwater solutions were used. For 10 days, 100 daily cycles of shutdown events were carried out along with additional permeate backpressure of up to 4 bar to improve the osmotic backwash (OB) cleaning. Each cycle consisted of 5 min filtration at 10 bar and 3 min pump-off (shutdown event). After the 100 cycles during the day, which was selected as a worst-case scenario and as an accelerated test of membrane damage due to shutdown events, the system was not in operation overnight (intermittent operation). According to the authors [47], the results showed no significant membrane performance deterioration after the 1000 starts/stops, indicating the robustness and reliability of the membranes and the spontaneous OB cleaning process.

It can be seen from the above bibliographic analysis, which is summarized in Table 1, that most of the experimental tests performed to date have considered the performance of BWRO desalination plants at laboratory scale. In addition, testing is generally carried out with a high percentage of the 24 h of a day in shutdown mode, trying to imitate plant performance when powered by a PV system with no operation between dusk and dawn. Except for [46], the tests have been limited to a few days. In addition, it should be noted that the very few tests performed to date with SWRO plants have been at laboratory scale, with the limitations that this implies, and, given their use of synthetic feedwater, have not considered the impact of actual raw water.

1.2. Aim, novelty and key contributions of this paper

The aim of this paper is to present the results of tests performed on an intermittently operating industrial SWRO desalination plant. The novel contribution of this work is that, for the first time, following a scientific method, a study is undertaken of the effects of intermittency on the membranes of a SWRO plant (with a 100 m^3/d capacity, fed with seawater pretreated with antiscalant, equipped with various sensors and an energy recovery system, and with forward flushing), using the baseline values of various parameters taken after a lengthy period of continuous plant operation and comparing them with the values obtained after intermittent plant operation with frequent starts/stops. In the experiments conducted, the operation of the various components comprising the desalination system was carried out using electrical energy from the conventional power grid. It should be noted that, regarding the energy source used for these experiments, our work does not differ from any of the studies previously conducted to analyze the effects of intermittent operation on membranes.

In wind-powered desalination systems that lack backup systems, the frequency of starts and stops primarily depends on the wind speed at the site, as well as the system configuration and the control strategy implemented. In this regard, to ensure that the start/stop frequencies are not influenced by the wind regime characteristics of the wind turbine installation site—which would result in outcomes heavily dependent on the specific wind regime and therefore not provide standardized reference results—this study, similar to the aforementioned prior works, establishes fixed start/stop frequencies. This approach avoids reliance on the stochastic nature of the energy source at a specific renewable energy installation site.

The key contributions of this paper are that it seeks to simulate an extreme operating situation of a wind-powered desalination system and proposes to model, using machine learning (ML) techniques, the importance of diverse input parameters of an SWRO plant and of its cumulative operating hours when estimating the target variables of normalized permeate flow (NPF), normalized salt rejection (NSR), normalized salt permeate concentration (NSPC) and normalized pressure differential (NPD). To analyse the difference between the values of the above parameters at the start and end of the test, use is made of statistical significance, denoted by p-values, and the effect size is estimated. Autopsies are also carried, through both external and internal inspections, to identify potential membrane damage. For the internal inspections, characterization and integrity tests are performed, as well as a membrane fouling analysis [48,49].

2. Materials

Fig. 2 shows a picture of the SWRO plant used in the tests. The picture is also available on the DESAL + LIVING LAB platform [50] which arose as an initiative of the DESAL + project (Interreg 2014–2020 MAC Programme), a fully-equipped public–private ecosystem located in the Canary Islands where, researchers, managers, technicians, businesses, water bodies and knowledge institutions can cooperate and investigate, develop, test and validate water desalination solutions based on the water-energy nexus and an RE approach.

The plant is installed inside a standard container measuring 2.35 x

Table 1
Summary of previous research work.

Paper	Aim	Technology	Scale	Feed water	Test duration	Operating pattern
Park et al. [39],	To investigate the impact of intermittent operation on permeate quality and quantity	BWRO	Laboratory	Prepared feed solutions	1 h	Six start/stop cycles
Freire-Gormaly and Bilton [40,41]	To compare the effects of intermittent vs. continuous operation	BWRO	Laboratory	Prepared feed solutions	3 days	8 h on, 16 h off per day
Sarker and Bilton [42]	To assess intermittent operation under high mineral scaling conditions (CaSO4)	BWRO	Laboratory	Prepared feed solutions	3 days	8 h per day
Kim et al.[43]	To examine biofouling under various synthetic saline groundwater conditions	BWRO	Laboratory	Prepared feed solutions	7 days	5 h on, 19 h off per day
Lee et al. [44]	To study fouling behaviour in pressurized RO membranes under intermittent conditions	BWRO	Laboratory	Prepared feed solutions	5 days	8 h on, 16 h off per day
Yang et al. [45]	To determine the impact of intermittent operation on membrane fouling	SWRO	Laboratory	Prepared feed solutions	2 days	Operating times varied from 4 to 14 h; three 3-hour shutdowns during testing
Ruiz-García and Nuez [46]	To analyse operating parameters and SEC evolution over long-term intermittent operation with consistent water production	BWRO	Full-scale	Brackish feedwater from an underground well	14 years	9 h/day continuous operation with nightly shutdowns
Cai et al. [47]	To evaluate membrane performance deterioration	BWRO	Laboratory	Synthetic brackish feedwater solutions	10 days	100 daily shutdown cycles; not operating overnight

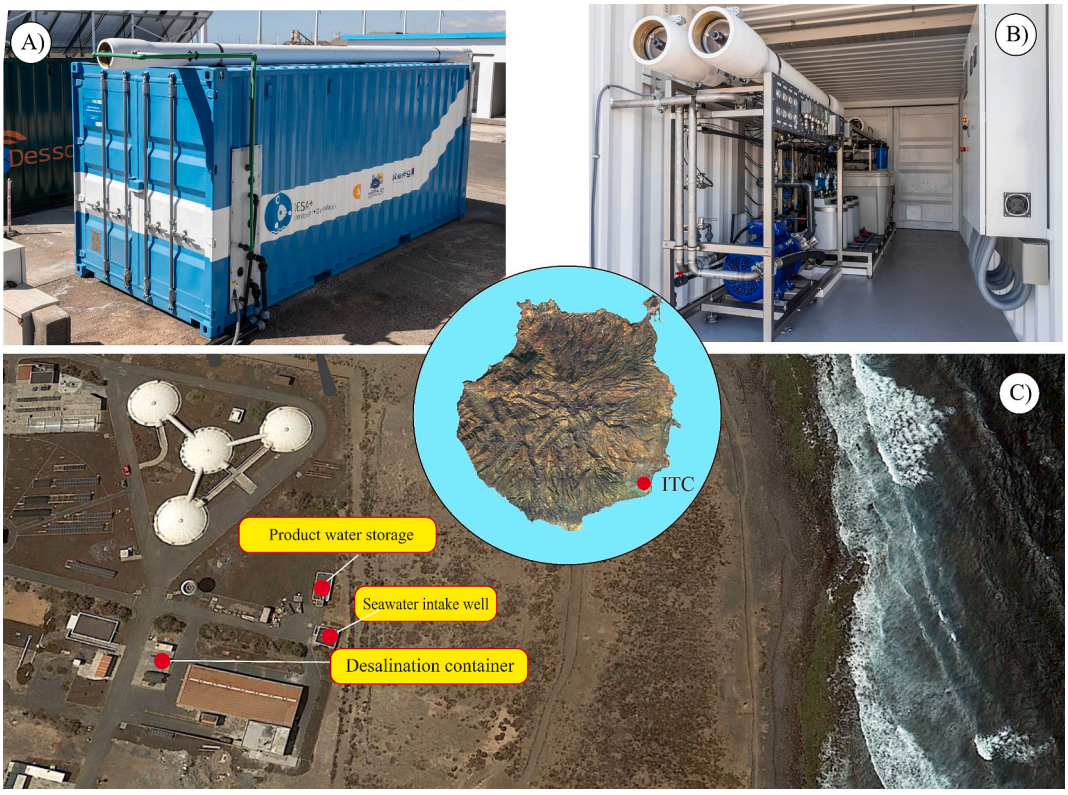

Fig. 2. A) Container housing the plant, B) Inside view of the container, C) Location of product water storage tank, seawater intake well and desalination plant container at the ITC premises.

5.90 x 2.39 m (W x L x H) located on the premises of the Canary Islands Institute of Technology (ITC by its initials in Spanish) on the island of Gran Canaria (Canary Islands-Spain). All seawater inlet and product and brine outlet connections are located on one side of the container and are duly marked. The seawater is collected by pumping the water from an intake well to the container (Fig. 2C). The pre-treatment of the SWRO plant feedwater comprises: a) a sand filter unit (with a flint bed of various grain sizes, with 0.6 m^2 of filter surface, a filtration flow rate of 10–12 m^3/h, and a filtration speed of 18 m/h); b) an antiscalant dosing unit (Vitec 3000® liquid antiscalant [51]) with a maximum flow rate of 3 L/h to prevent the incrustation of sulphate and carbonate salts on the membrane surfaces (dosage, dependent on the ionic components of the seawater and the SWRO reject, set at 2 ppm); and c) two filter housings, each with a cartridge filter unit (10 μm absolute and 508 mm long) made of polypropylene and with a 100 mbar cartridge pressure drop (Fig. 3).

The tank volume of the cleaning and flushing equipment is 500 L. When the forward flushing equipment is operated, the seawater content remaining on the membranes is displaced with water produced by the SWRO in order to remove the layer of contaminants built up on the membrane by creating turbulence.

The 22 kW electric motor that drives the high-pressure pump and energy recovery device (SALINO 120 [52]), although it has a variable frequency drive, is set to a constant speed of 750 rpm. The nominal flow rate of the high-pressure pump is 10.42 m^3/h, and the maximum operating pressure is 53 bar. The SWRO plant consists of two pressure vessels in series (Fig. 3). The first has 5 membranes and the second 2. The spiral-wound composite polymer membranes (Hydranautics model SWC4-LD for seawater [53]) have a maximum operating temperature of 45 °C, a pH range of 4–11, a diameter of 200 mm and length of 1,016 mm, a membrane active area of 37.1 m^2, and a 99.8 % salt rejection rate.

3. Experimental method

Fig. 4 shows a block diagram synthesizing the method used and the tasks associated with the test.

Among the various schedules carried out in Task-1 is the definition of the intermittency cycle in the operation of the SWRO plant. In this context, the SWRO is first programmed to operate continuously for a period of slightly over 7 days (174 h). The parameter values obtained are then used as baseline values when estimating the NPF, NSR, NSPC and NPD values of the intermittency test. Baseline system performance values are useful for showing any performance changes between continuous operation and a given time of intermittent operation. That is, it is only possible to determine whether the change in performance is apparent or real by comparing the “normalized” intermittent operation performance data with baseline reference performance data.

In wind-powered desalination systems that do not employ backup systems, the frequency of starts/stops depends on the wind regime at the site, the system configuration and the control strategy employed. Carta and Cabrera [21], when simulating the long-term (19 years) operation of 8 SWRO modules with a 1,000 m^3/d capacity and following the strategy used in the SDAWES project [22], obtained an annual maximum number of starts/stops of the SWRO modules ranging between 550 and 600 (Fig. 5). This corresponds to a mean number of daily starts/stops ranging between 1.5 and 1.6. In this work, it was decided to substantially increase the number of starts/stops in order to simulate an extreme situation. In this context, it was determined that the plant would operate for 1 h followed by 1 h of shutdown. In other words, each day the plant would be in operation for 12 h and be shut down for the other 12.

The variable frequency drive is programmed so that the rotational speed (and consequently the seawater flow rate feeding the high-pressure pump) increases over time following three ramp functions, with two constant steps (at speeds of 100 rpm and 200 rpm), until reaching the nominal operating speed of 750 rpm (Fig. 6).

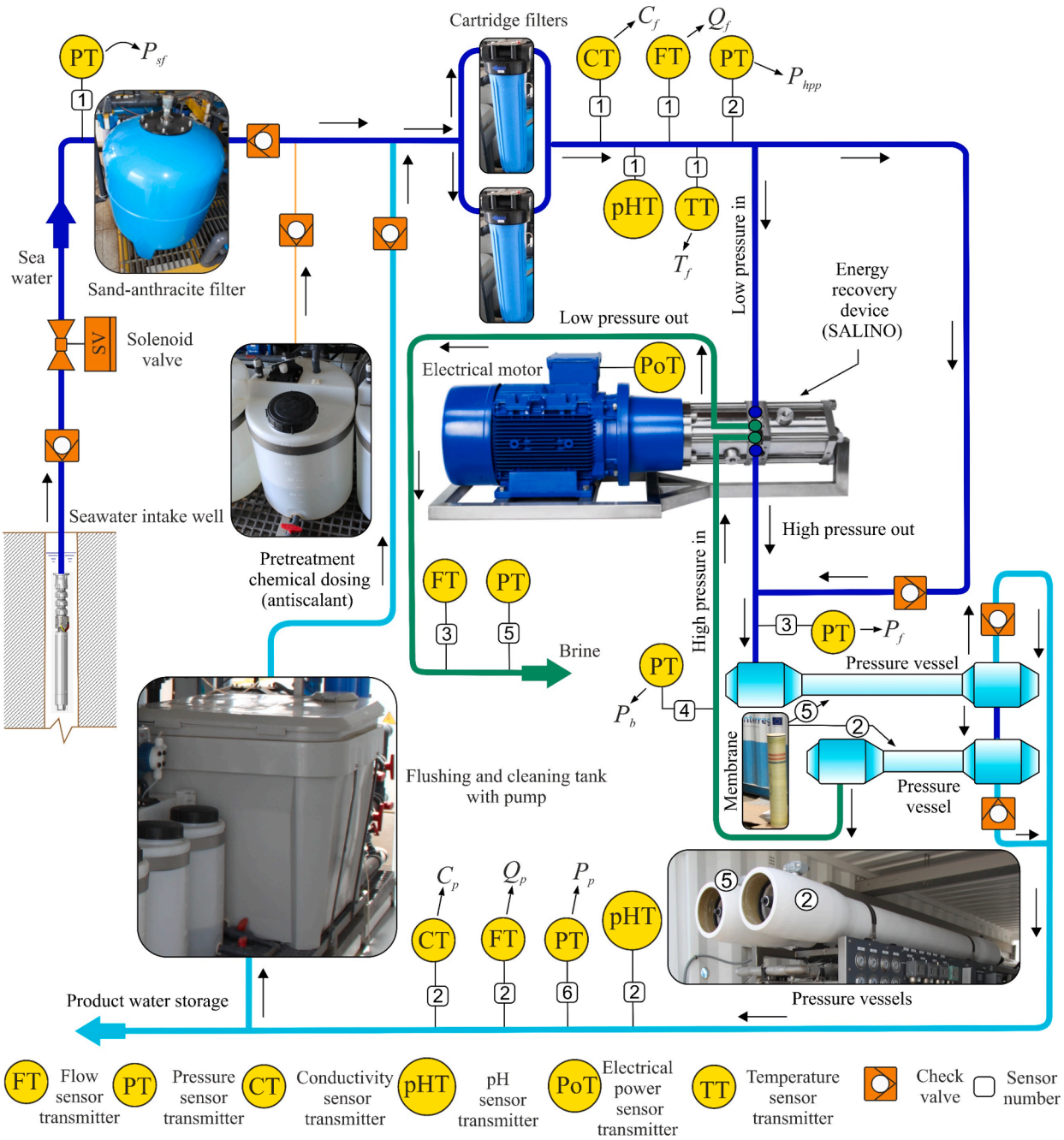

Fig. 3. Schematic outline of the general configuration of the used system.

Based on the assumption that a one-hour shutdown of the SWRO plant is short, that the water comes from an intake well, that the system has a sand filter and cartridge filters and that the water is pre-treated with antiscalant before being fed to the membranes, it was decided that the washing equipment would not be activated during the one-hour shutdown period and would only be activated if, for any reason, the shutdown period were longer than 1 h.

The frequency of data collection was set in Task-1 at 1 s^{-1}. In Task-4, the SWRO plant test is started. If feed pressure or feed flow rate ramps up too fast, the elements can be damaged by excessive forces in the flow or radial direction – especially if there is air in the system – which would cause a telescoping effect and/or breakage of the fibreglass wrap. To avoid the effects of rough start-ups on the membranes, instead of using a motorised solenoid valve at the outlet of the high-pressure pump that would allow a gradual increase in the pressure on the membranes, as was done in the SDAWES project [23], in the prototype tested in the present study the input flow is controlled through the variable frequency drive.

This procedure ensures that the SWRO system is pressurized at no more than 0.69 bar per second, as recommended by the manufacturers [54,55], and that therefore no damage is done to the membrane element. The recorded parameters are the cumulative operating time of the test (t_0) and the measures taken by the sensors shown in Fig. 3. For the entire system, the NPF, Eq.(1), and the NSR, Eq.(2), are calculated following ASTM Standard D4516[56,57], but taking salt passage, SP_a, as the ratio between permeate concentration and average feedwater concentration, as usually considered by membrane manufacturers in their manuals [58–60].

Although there is no specification for NSPC and NPD in ASTM D4516, some membrane manufacturers implement a version based on

Fig. 4. Block diagram of the tasks performed.

element-specific conditions. In this context, Eq.(3) [61,62] and Eq.(4) [62,63] were used, respectively, previously employed by Farhat *et al.* [62], in a two-stage RO plant.

$$NPF = Q_{pa}\frac{P_{fr} - \frac{\Delta P_{fbr}}{2} - P_{p_r} - \pi_{fb_r} + \pi_{P_r} TCF_r}{P_{f_a} - \frac{\Delta P_{fba}}{2} - P_{p_a} - \pi_{fb_a} + \pi_{P_a} TCF_a} \quad (1)$$

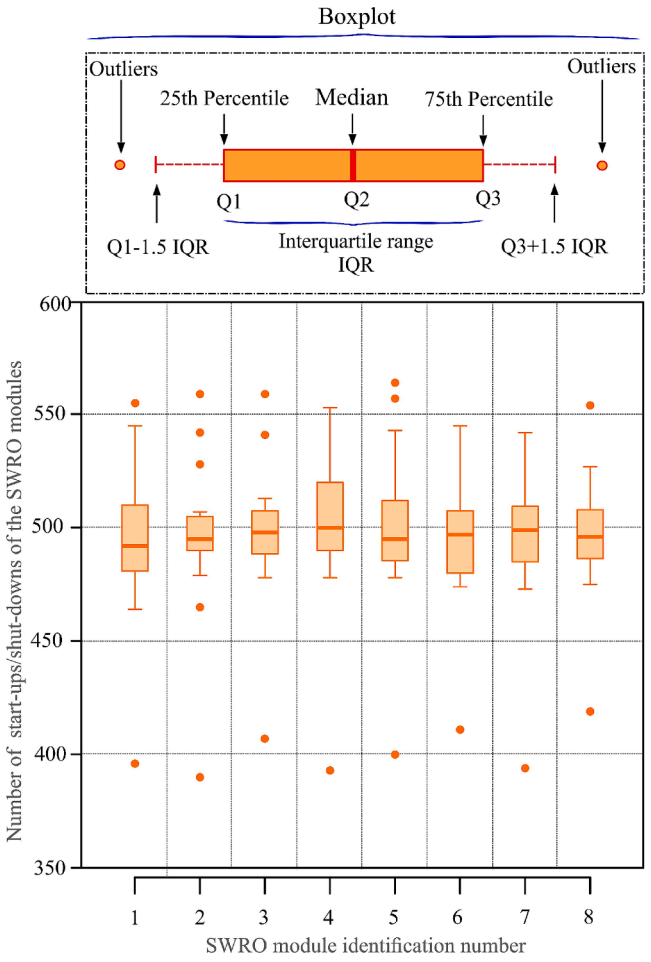

Fig. 5. Annual number of start-ups/shutdowns of the 8 SWRO modules [22].

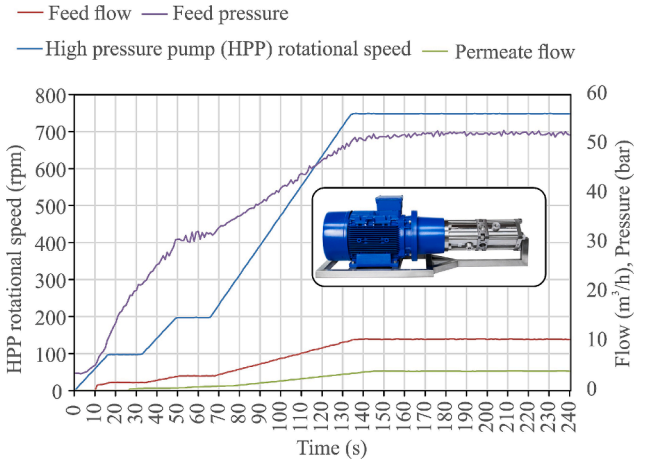

Fig. 6. Gradual increase of membrane pressure during the start-up periods.

$$NSRN = 100 - \frac{Q_{p_a}}{Q_{p_r}}\frac{STCF_r}{STCF_a}\frac{C_{fb_r}}{C'_{fb_a}}\frac{C_{f_a}}{C_{f_r}}(100 \cdot SP_a) \quad (2)$$

$$NSPC = \cdot Cp_a \cdot \frac{P_{f_a} - \frac{\Delta P_{fba}}{2} - P'_{p_a} - \pi_{fb_a} + \pi_{p_a}}{P_{f_r} - \frac{\Delta P_{fbr}}{2} - P_{p_r} - \pi_{fb_r} + \pi_{p_r}} \cdot \frac{C_{fb_r}}{C_{fb_a}} \quad (3)$$

$$NPD = \Delta P_a \cdot \frac{\left(2 \cdot Q_{f_r} - Q_{p_r}\right)^{1.5}}{\left(2 \cdot Q_{f_a} - Q_{p_a}\right)^{1.5}} \quad (4)$$

In the above equations, the subscripts '*a*' and '*r*' refer to the actual and reference (baseline) measurement values. The variables of the equations are described in the nomenclature and the expressions employed to estimate some of them are shown in the Supplementary Material.

In Task-5, once the test has been completed, the training, validation and testing of the four ML models (for NPF, NSR, NSPC and NPD) is carried out (Fig. 7). The models are expected to learn, in a supervised way, the relationship between the operating time (t_o) and certain operating variables of the SWRO plant (P_{hpp}, P_f, Q_f, T_f, C_f, P_p, $P_p = P_{sf}$-P_{hpp}, $Y = Q_p/Q_f$), used as input variables to the model, and the defined target variables (NPF, NSR, NSPC and NPD).

In this work, the regression function given in Eq.(5) is estimated using the random forest (RF) technique, proposed by Breiman [64]. In previous studies, it has been found to provide appropriate metrics against other ML techniques [21,65]. It was selected for the present study in view of its robustness against overfitting.

$$\left.\begin{matrix} NPF \\ NSR \\ NPD \\ NSPC \end{matrix}\right\} = f\left\{ (P_{hpp})_t, (P_f)_t, (Q_f)_t, (T_f)_t, (C_f)_t, (P_p)_t, (\Delta_p)_t, (Y)_t, (t_o)_t \right\} \quad (5)$$

The randomForest package [66] of the open-source multi-platform R Statistics software [67] was used to programme the proposed model.

The procedure followed (Fig. 7) is similar to that used in [17]. After concluding the training and validation of the RF model with the best hyperparameters, the permutation feature importance measurement introduced by Breiman [68] for RFs is used to determine the variables most important to the model.

After the RF model has been defined, its testing is undertaken using the predict() function, available in the randomForest package [66] of the R Statistics software, and the test subset as its input data. The proposed metrics for the subsequent analysis are the root mean square error (RMSE)[69], the mean absolute error (MAE) [22,69] and the adjusted coefficient of determination (R^2) [21] (see Supplementary Material).

Membrane autopsy is performed in Task-6, as this is one of the most useful tools for the identification of potential membrane damage [46,47]. Fig. 8 schematically represents the proposed analyses and tests to be undertaken in the autopsies of the first and last membranes of the system.

4. Results

Shown in Fig. 9 is the evolution of various operating parameters of the SWRO desalination plant over the 174 h that comprised the continuous operation test period. The mean values of these parameters are also shown. The values recorded in the last hours of operation of this test were used as baseline values in the analysis of the evolution of these parameters in the intermittent operation test.

Fig. 10 shows the evolution of the values of the target parameters (NPF, NSR, NPSC and NPD) obtained over the 3,136 h (1,568 h of operation and 1,568 h of shutdown) of intermittent operation. The x-axes represent the cumulative hours of operation, t_o. Also shown are the results of the inferential statistical analysis (hypothesis testing) made with the 36-h data samples (equivalent to 3 days of intermittent operation) collected at the beginning and end of the intermittent operation

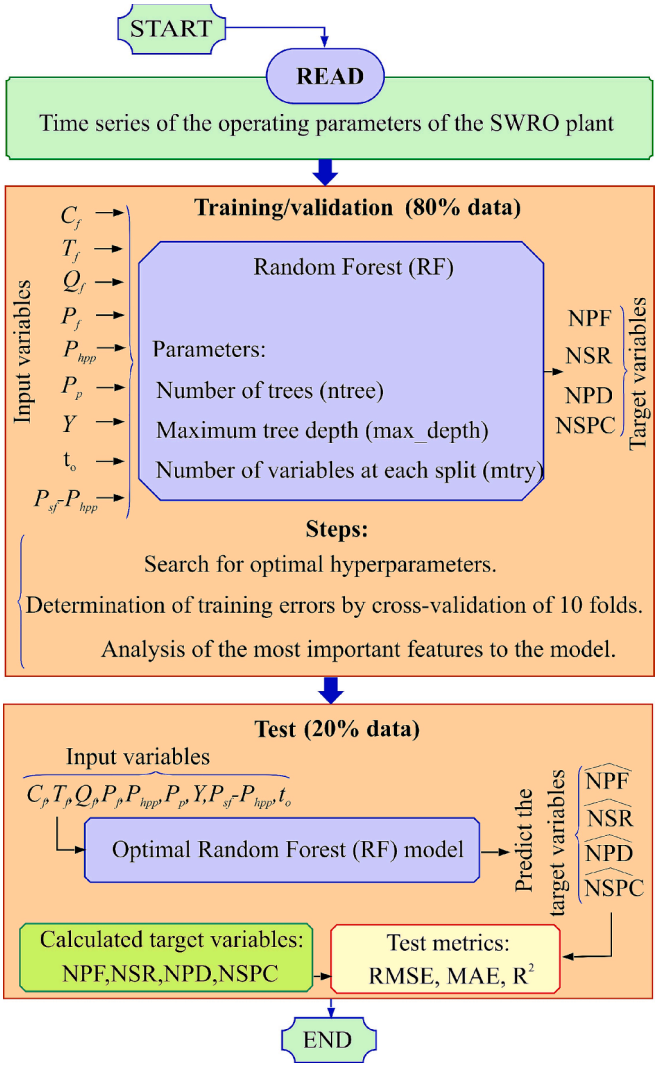

Fig. 7. Schematic representation of the fifth task of the method employed.

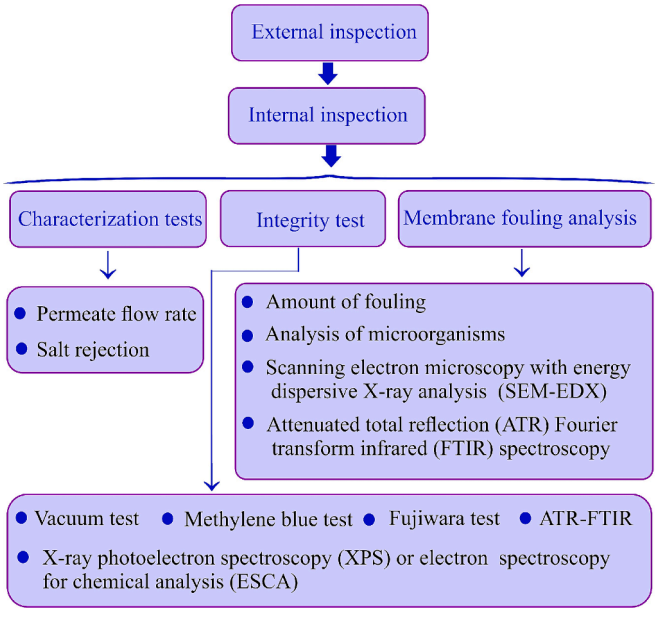

Fig. 8. Schematic representation of the proposed membrane autopsy analyses and tests.

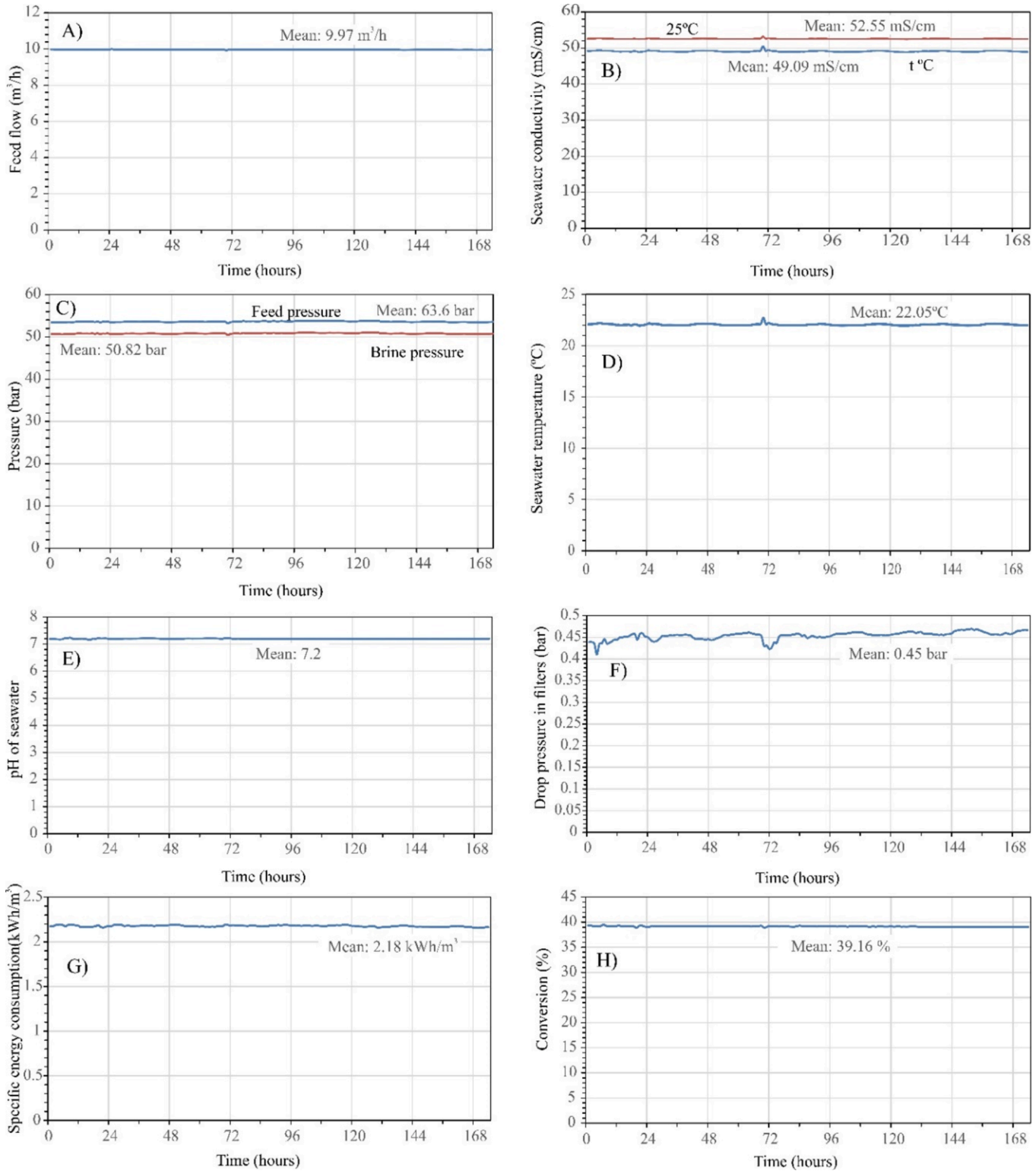

Fig. 9. Evaluation of SWRO plant parameters vs. operating time in the continuous test.

test. The sample size of 36 h was chosen as 30 is often used as a general rule for a minimum sample size as it is the point at which the central limit theorem begins to be applied [70]. The paired hypothesis tests aimed to test for the existence or otherwise of statistically significant differences before and after the intermittency test. Prior to choosing the way to carry out these hypothesis tests, the Shapiro-Wilk test [71] was used to check whether the sample differences used could be accepted as coming from a population with a normal probability distribution.

The p-values were above 0.05 (previously established significance level) for all mean differences, indicating insufficient evidence to reject the null hypothesis of normality.

The Student's *t*-test [72] and, in the case of the presence of outliers, the robust Yuen test [73] were used to carry out the hypothesis tests. Fig. 10 also shows the effect size[74,75] of the intermittent test using the

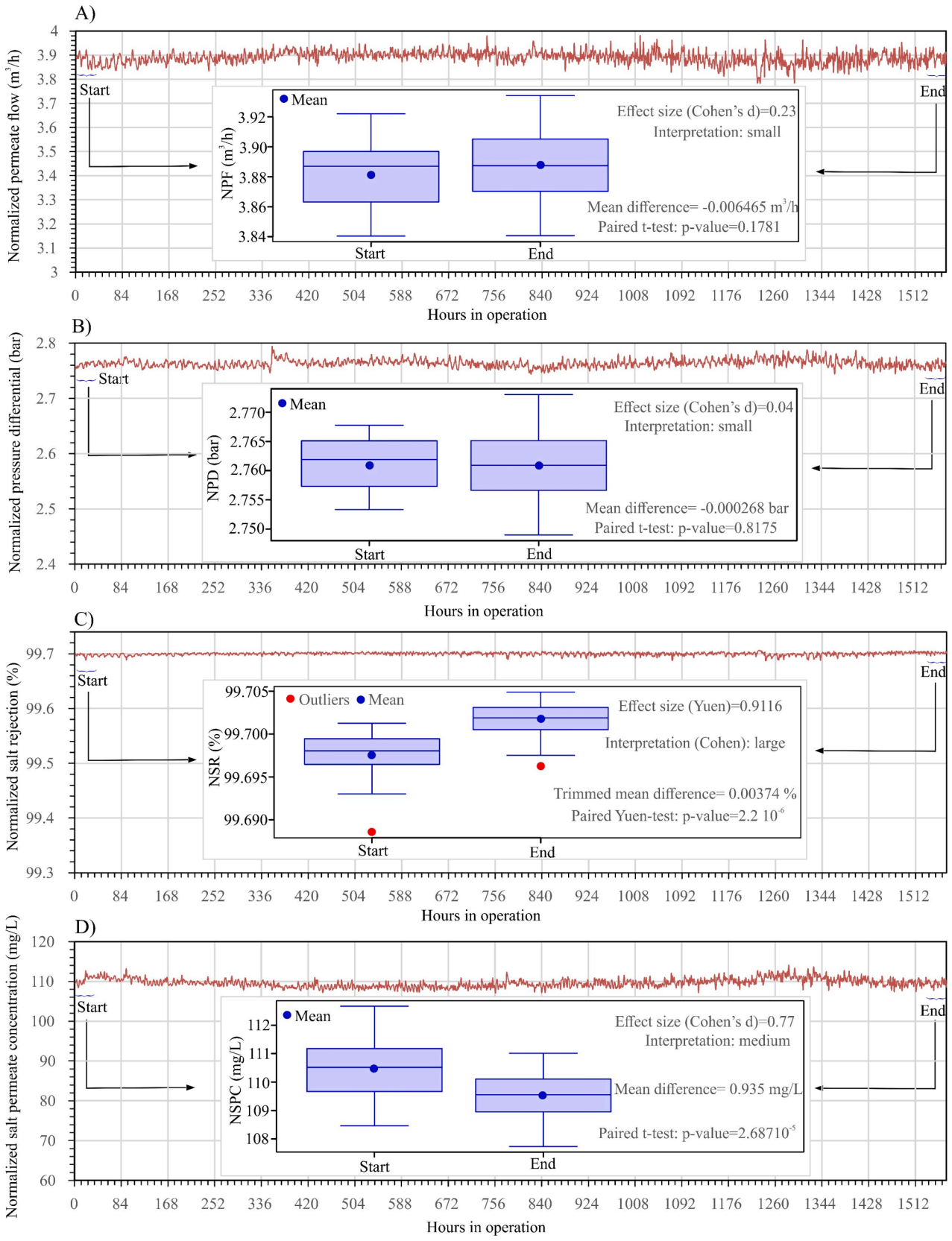

Fig. 10. Evolution of the normalized parameters of the SWRO plant vs. cumulative operating time (t_o) in the intermittent test. Boxplots of 36 h of operation at the start and end of the intermittency test. Statistical tests and effect size.

sample data, which is intended to assess the magnitude of the observed differences between the variables and thus complement the statistical inference analysis, which only assesses the direction of the effect [73] (i.e. it does not clearly indicate how much the groups differ [75]). Standardised measures were used to interpret effect sizes. The conventional effect sizes proposed by Cohen [76] are 0.2 (small effect), 0.5 (medium effect) and 0.8 (large effect).

Fig. 10 shows the results of the four RF models used to estimate the normalized parameters. The first column (Fig. 10 A-D) shows the optimal hyperparameters of the models and the values of the metrics used in their evaluation. The second column (Fig. 11 E-H) shows what in machine learning terminology is known as variable importance[77]. Importance was measured with the factor %IncMSE. This factor represents the mean decrease of the accuracy of the predictions about the samples not used to fit each tree of the forest when the given variable is excluded from the model. The predictors that are more important will correspond to those with higher %IncMSE. Fig. 11 shows the values of the parameters C_f, T_f, P_{hpp} and P_f during the 3,136 h of intermittent operation. As in Fig. 10, the x-axes represent the cumulative hours of operation, t_o. Also shown are the results of the inferential statistical

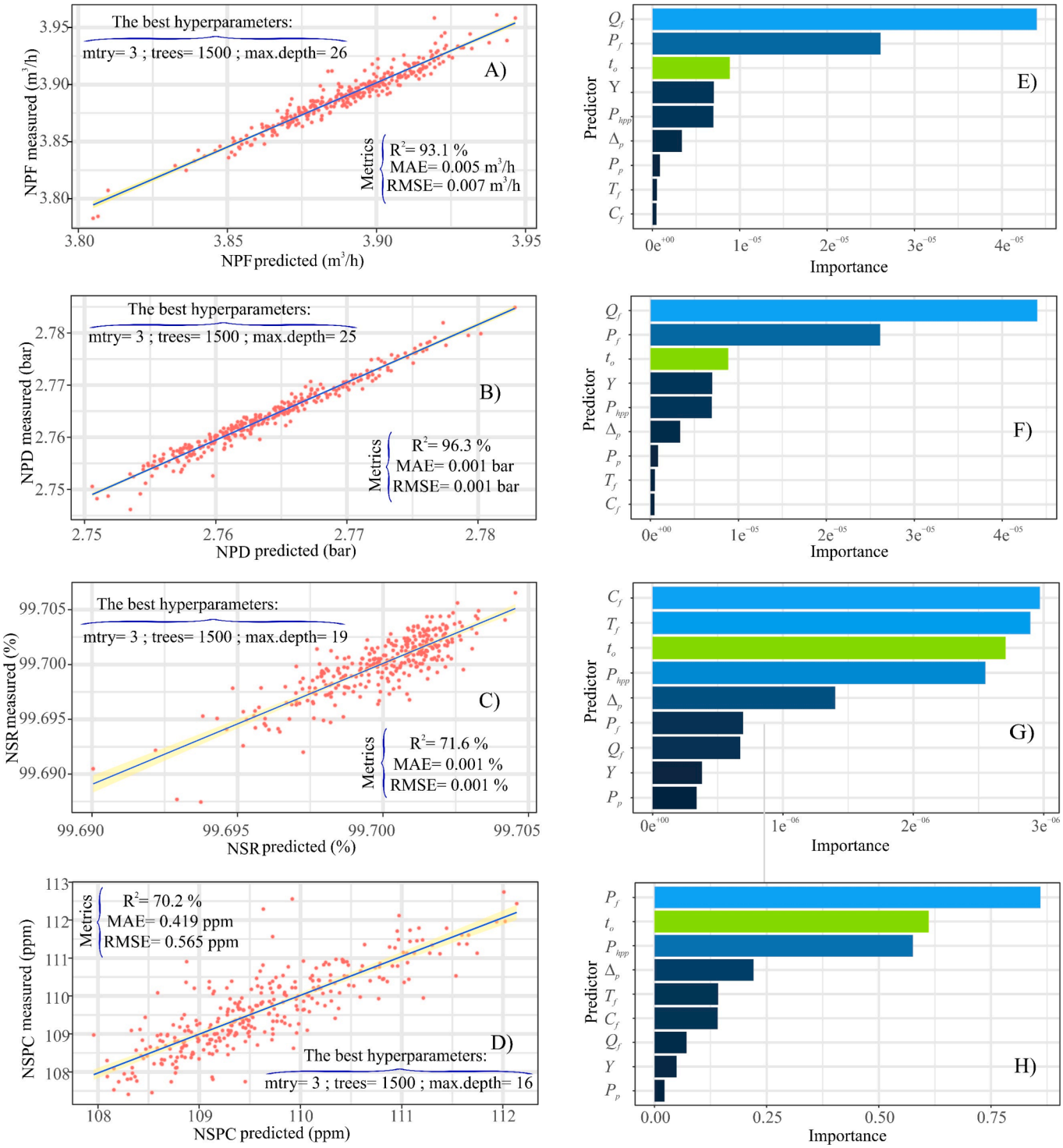

Fig. 11. Results obtained with the RF models. From A) to D) hyperparameters and metrics. From E) to H) importance of variables used in RF modelling.

analysis made with the 36-h samples of data collected at the beginning and end of the intermittency test, and the effect size [74,75].

Table 2 provides a summary of the results obtained with the autopsies performed on the two membranes (see Supplementary Material).

Fig. 13 shows a summary of the statistical results and their relationship with the biophysical results. This figure illustrates the existence of a cause-and-effect relationship between the statistical results and the physical results.

5. Discussion

This study investigates the effects of continuous and intermittent operation with frequent start-stop cycles on the performance and integrity of SWRO membranes. The discussion is structured to first present the findings from continuous operation, followed by an analysis of intermittent operation, emphasizing technical and scientific insights.

5.1. Continuous mode operation

The continuous operation test provided a stable baseline for assessing the performance of the SWRO plant under steady-state conditions. As depicted in Fig. 9, key operational parameters—including feed flow, conductivity, pressure, temperature, pH, pressure drop across filters, specific energy consumption, and conversion rate—exhibited consistent trends throughout the 174-hour test.

The feed flow averaged 9.97 m3/h, reflecting reliable operation of the high-pressure pump and energy recovery device. Similarly, the feed and brine pressures remained stable, averaging 63.6 bar and 50.82 bar, respectively, indicating efficient hydraulic stability. Feedwater quality showed minimal variability, with conductivity averaging 52.55 mS/cm and temperature at 22.05 °C. The stable feedwater pH of 7.2 and low pressure drop across the filters, which averaged 0.45 bar, ensured consistent osmotic pressure and optimal membrane operation. The system's specific energy consumption averaged 2.18 kWh/m3, highlighting its energy efficiency, while the average conversion rate of 39.16 % reflected steady and predictable permeate production. The consistent performance across these parameters validates the robustness of the SWRO plant under continuous operation.

Graphical annotations in Fig. 9 illustrate how stable feedwater properties, such as conductivity and temperature, directly supported optimal system performance and energy efficiency. These findings provide a reliable baseline for evaluating the impacts of intermittent operation, discussed below.

Table 2
Results of the analysis carried out in the membrane autopsies.

Analysis	First membrane	Last membrane
External inspection	No detection of vexar feed spacer displacement or telescoping effect.	No detection of vexar feed spacer displacement or telescoping effect.
Internal inspection	**Visual inspection**	
	Marks were detected from the spacing material in the area furthest from the permeate tube. Presence of particles at the feed end of the spacer material.	As in the first membrane, marks were detected on the membrane surface caused by the spacing material.
	Microscopy inspection	
	Scant presence of membrane surface fouling. Abrasion marks detected at high magnification.	Abrasion marks detected at high magnification.
Fouling identification	No significant fouling on the membrane surface. Sodium chloride (0.05 mg/cm^2). Aluminosilicate, potassium and magnesium particles.	No significant fouling. Sodium chloride (0.06 mg/cm^2). Aluminosilicate, potassium and magnesium particles.
Integrity and oxidizations tests	Vacuum test negative. Damage detected to the polyamide layer (methylene blue test positive).Fujiwara test negative and the presence of halogens not detected by XPS.	Occasional damage detected to the polyamide layer (methylene blue test positive). Fujiwara test negative and the presence of halogens not detected by XPS.
	No changes detected in the polyamide bands by internal reflection spectrometry (IRS).	No changes detected in the polyamide bands by IRS.
Operating parameters	Permeate flow: above the benchmark value established by the manufacturer.Salt retention: Slightly lower than the minimum value determined by the manufacturer.	Permeate flow: above the benchmark value established by the manufacturer. Salt retention: within the minimum interval determined by the manufacturer.

5.2. Intermittent mode operation

The intermittent operation test subjected the SWRO plant to 1,568 start-stop cycles over a total duration of 3,136 h, with alternating 1-hour operating and shutdown periods. This test was designed to simulate extreme operational scenarios associated with the variability of renewable energy sources such as wind power.

Throughout the test, the NPF exhibited a slight, statistically insignificant increase of 0.0065 m^3/h (p-value = 0.1781; effect size = small), indicating that the system maintained permeability without significant fouling or scaling. Similarly, the NPD showed no significant changes (p-value = 0.8175; effect size = small), confirming that frequent start-stop cycles did not result in increased flow resistance or clogging, Fig. 13.

Conversely, the NSR demonstrated a statistically significant improvement (p-value < 0.001; effect size = large), reflecting enhanced salt rejection and higher permeate quality. This improvement is likely due to biofouling material sealing minor membrane imperfections, as corroborated by the minimal fouling observed during membrane autopsies, Fig. 13. Additionally, the NSPC decreased significantly (p-value < 0.001; effect size = medium), indicating reduced salt diffusion into the permeate water, Fig. 13. These changes, as indicated by the warning symbol in Fig. 13, were influenced by reductions in feedwater conductivity (527 mg/L) and temperature (1.2 °C), as shown in Fig. 12A, B, which lowered osmotic pressure and enhanced salt rejection efficiency.

According to Kim *et al.* [43], intermittent operation could compensate for physical cleaning. However, in this work, without discarding the conclusion of these authors [43], it is considered that justification for the decrease in NSPC can be supported by two reasons: a) that there is a slight increase in NPF; and b) that less salt diffuses and dissolves in the same or more product water. The rate of salt passage is independent of pressure [37]. However, because the same or more permeated water is produced, the NSPC decreases. It is estimated that this occurs because less salt diffuses across the membrane, but dissolves in the same or more permeated water.

The machine learning RF models constructed to estimate NSR and NSPC achieved R^2 values of 71.6 % and 70.2 %, respectively, indicating good predictive accuracy. The primary predictors for NSR were feedwater conductivity C_f, temperature T_f, operating time t_o and and inlet pressure to the high-pressure pump P_{hpp}. Similarly, NSPC predictions predictions were influenced by feed pressure P_f, and inlet pressure to the high-pressure pump P_{hpp}. The models confirm that changes in these parameters directly impacted membrane performance during intermittent operation. The variable t_o occupies second position among all the predictors used in the model.

The stability of NPF and NPD, combined with the improvements in NSR and NSPC, highlights the system's resilience under frequent start-stop cycles.

The membrane autopsies, presented in Table 1 (and Supplementary Material section 4), further support these findings, revealing only minor physical wear and isolated fouling deposits, which did not significantly impact performance. It should be noted that three samples were taken from each of the two autopsied membranes and the permeate flow rate

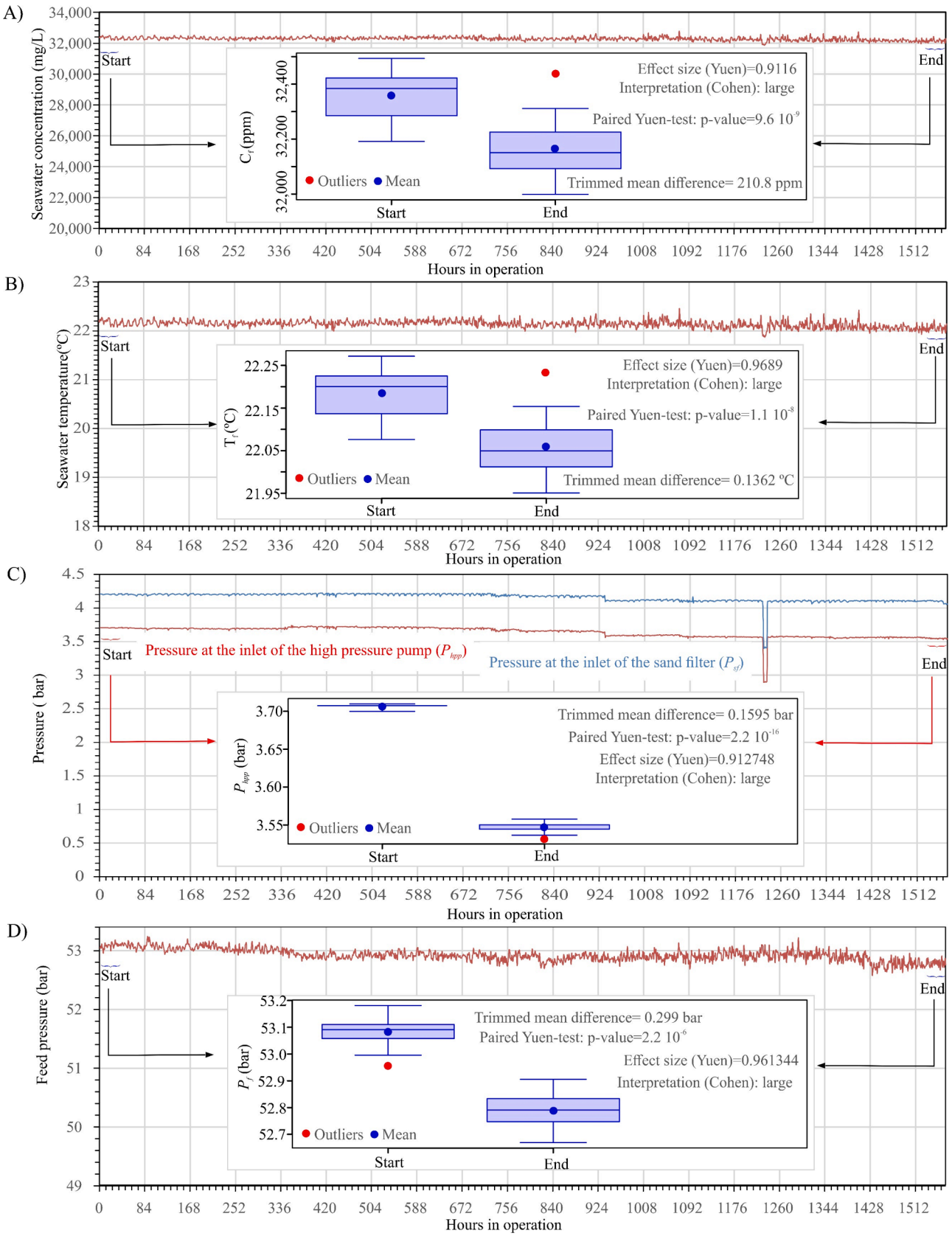

Fig. 12. Evolution of certain parameters vs. cumulative operating time (t_o) in the intermittent operating period of the test. Boxplots of 36-h of operation at the start and end of the intermittency test. Statistical tests and effect size.

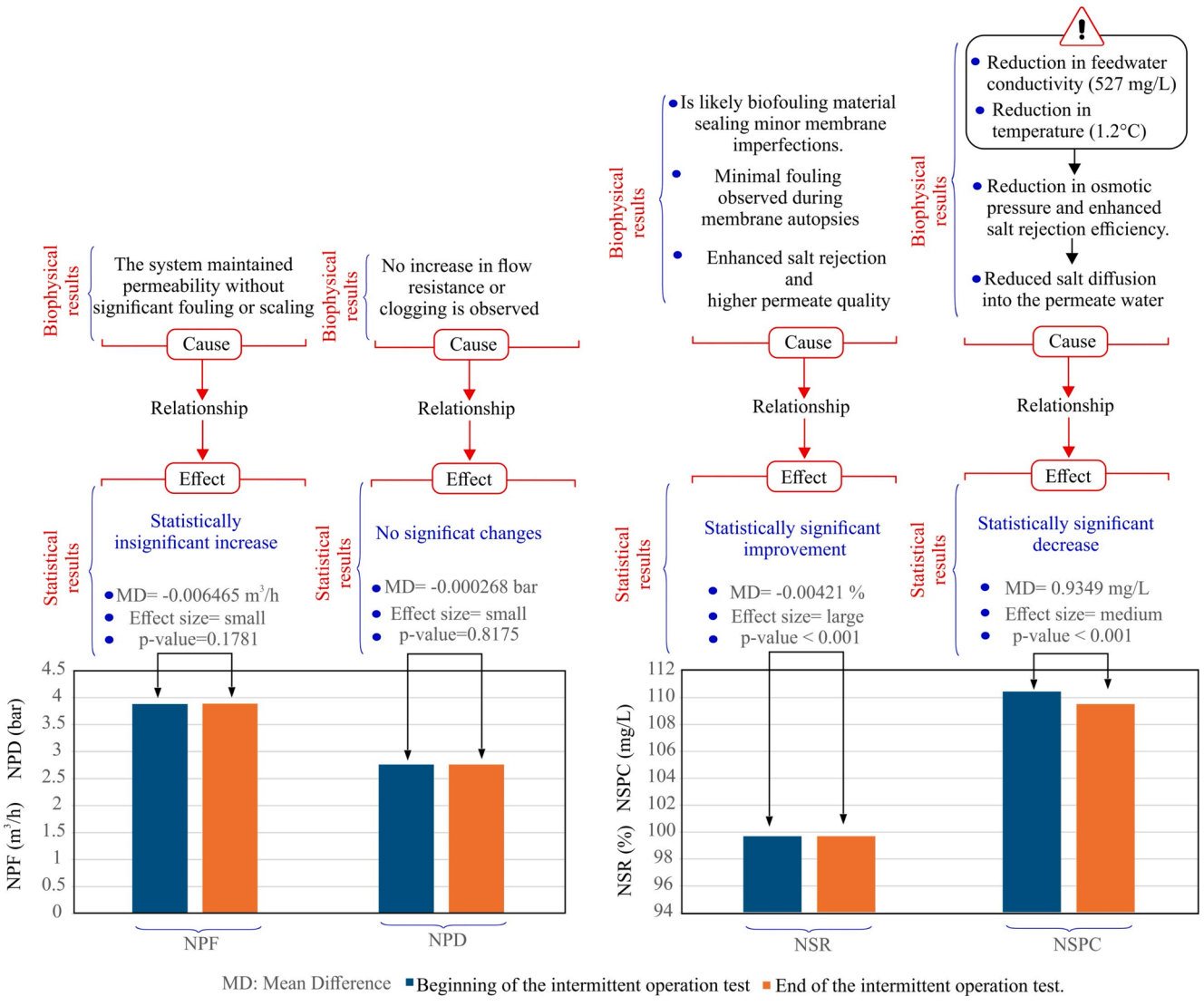

Fig. 13. Cause-and-effect relationship between the statistical results and the biophysical results.

and salt retention in the flow cell were characterised. For the characterisation of the operating parameters of the samples, the standard conditions established by the manufacturer of the autopsied membranes were taken into account. As can be seen in Table 1, the mean permeate flow rate value at 25 °C of both membranes was above the design value established by the manufacturer, which is usually characteristic of damaged membranes. Despite this, salt retention did not appear to be greatly affected in the operating parameter tests (Table 1) or in the recorded NSR evolution (Fig. 10C)), as the value is within the range established by the manufacturer (99.7 %-99.8 %).

It should be noted that a membrane is generally considered 'bad' when salt rejection drops to 90 % or less [78]. As reported in Table 2, no telescoping effects were detected in the membranes, but vexar displacement was detected at the rejection end. That is, displacement of the netting material placed between the flat sheets of a SWRO membrane was found to promote turbulence in the feed/concentrate stream. In fact, internal inspection revealed marks on the membrane surface caused by the spacer material in the area furthest from the permeate tube and the methylene blue test indicated damage to the polyamide layer (see Supplementary Material). However, this damage was not reflected in the evaluation of the parameters measured in the system.

As shown in Table 2, the microscopy inspection concluded that the surface of the membranes showed hardly any fouling, just a few isolated deposits/particles in certain areas. These particles/fouling had an amorphous morphology/structure. However, at high magnification, abrasion marks were detected. Although no oxidation processes were confirmed on the membranes, traces of chlorine in the form of C-Cl were found on the membrane in the first position. Graphical annotations in Figs. 10 and 12 provide a clear visualization of the relationships between operating parameters and system performance, illustrating how changes in feedwater properties and pressure directly influenced permeate quality and salt rejection.

In should be noted that, in the configuration of the systems used (Fig. 3), it would have been appropriate to install monitoring devices between the two pressure vessels to carry out a more detailed normalization. In particular, it would have been advisable to install flow, pressure and conductivity sensors at the permeate outlet of the 1st pressure vessel and the water inlet of the 2nd pressure vessel. For example, if NPD had been measured at each pressure vessel, differentiation between fouling and scaling could probably have been made based on the location of an increase in the pressure drop. An increase in NPD in the first pressure vessel would indicate fouling issues and an increase in NPD in the second pressure vessel would indicate scaling issues.

According to the normalised data analysis performed, the results seem to reflect the resilience of the process after 1,568 starts/stops, using pretreatment, but not osmotic backwash (OB) cleaning. Graphical

annotations in Figs. 10 and 12 highlight the relationships between operating parameters and system performance. For instance, the improvements in NSR and NSPC are closely linked to stable feedwater conditions and slight reductions in conductivity and temperature. These results confirm the system's ability to adapt to intermittent operation without significant performance degradation. With respect to the latter, it should be noted that Cai *et al.* [47] pointed out that a periodic cleaning strategy is effective in mitigating contamination in RO spiral wound modules. However, they also reported that very frequent OB cleaning, combined with chemical cleaning, could accelerate membrane deterioration.

The findings discussed underscore the resilience of the SWRO system under intermittent operation, providing valuable insights into the feasibility of wind-powered desalination systems. However, further optimization is needed to mitigate long-term wear, particularly through improved cleaning protocols and enhanced monitoring systems. Installing additional sensors for flow, pressure, and conductivity between pressure vessels could facilitate more detailed diagnostics, distinguishing between fouling and scaling more effectively.

To build upon these findings, future research should explore longer test durations and varied intermittent patterns to better understand cumulative effects on membrane integrity and develop strategies to enhance system longevity.

6. Conclusions

In this work, a study was carried out on the effects on the membranes of a SWRO desalination plant with a capacity of 100 m^3/d operating firstly in continuous mode for 174 h and then in intermittent mode with frequent starts/stops. The aim with the latter mode was to simulate an extreme case of the operation of a wind-powered SWRO desalination plant.

The main findings can be summarized as follows:

- According to the analysis of the normalised data, the results seem to reflect the resilience of the process after 1,568 starts/stops, using pre-treatment, but not osmotic backwash cleaning.
- No statistically significant differences were found between the mean values at the beginning and at the end of the test for the NPF and NPD parameters. Therefore, it was considered that no fouling or scaling was present on the membranes. The NPF increased slightly (0.006465 m^3/h), and so it could be conjectured that damage to the membranes had occurred. However, this was not evident in the statistical analysis.
- It was observed that NSR increased and NSPC improved at the end of the intermittency test. It is considered that the increase in NSR is not a consequence of biological contamination, as no decrease in NPF was detected. It is considered that the justification for the increase in NSR can be supported by the decrease in operating parameters such as feedwater temperature and conductivity.
- The t_o variable was in the top variable importance positions of all the predictors used in the RF models to estimate NSR and NSPC. Although it has been pointed out in the literature that intermittent operation, captured by t_o, could compensate for physical cleaning, in this work it is considered that the decrease in NSPC can be justified by the slight increase in NPF and the lower diffusion of salt that dissolves in more product water.
- With respect to the results obtained with the autopsies, it should be noted that both membranes presented a permeate flow rate above the design value, which is usually characteristic of damaged membranes. Despite this, salt retention did not appear to be greatly affected in the operating parameter tests, as the value was within the range established by the manufacturer.
- No telescoping effects were detected on the membranes, but marks on the membrane surface caused by the spacer material were detected in the area furthest from the permeate tube and the methylene blue test indicated damage to the polyamide layer. However, this damage was not clearly reflected in the evaluation of the parameters measured in the system.
- The microscopy inspection concluded that the surface of the membranes showed hardly any fouling, only isolated deposits/particles in certain areas. Although no oxidation processes were confirmed on the membranes, traces of chlorine in the form of C-Cl were found on the membrane in the first position.
- It would be advisable to install flow, pressure and conductivity sensors at the permeate outlet of the 1st pressure vessel and at the water inlet of the 2nd pressure vessel in order to carry out a more detailed normalisation. It is also considered that, to obtain more conclusive results, it would be advisable to carry out tests over a longer period.

CRediT authorship contribution statement

José A. Carta: Writing – original draft, Visualization, Validation, Supervision, Software, Resources, Methodology, Investigation, Formal analysis, Data curation, Conceptualization. **Pedro Cabrera:** Writing – original draft, Visualization, Validation, Supervision, Resources, Project administration, Methodology, Investigation, Funding acquisition, Formal analysis, Data curation, Conceptualization. **Noemi Melián-Martel:** Resources, Investigation, Formal analysis, Data curation. **Sigrid Arenas-Urrea:** Resources, Investigation, Data curation.

Declaration of competing interest

The authors declare that they have no known competing financial interests or personal relationships that could have appeared to influence the work reported in this paper.

Acknowledgements

This research is part of the project PID2022-142148OA-I00 funded by MCIN/AEI/10.13039/501100011033/FEDER, UE. The work has been co-funded by INTERREG MAC 2021-2027 program, within the IDIWATER project (1/MAC/1/1.1/0022), who is integrated in the DESAL + Living Lab Platform (desalinationlab.com).

Appendix A. Supplementary data

Supplementary data to this article can be found online at https://doi.org/10.1016/j.ecmx.2024.100848.

Data availability

The authors do not have permission to share data.

References

[1] Alawad SM, Ben Mansour R, Al-Sulaiman FA, Rehman S. Renewable energy systems for water desalination applications: a comprehensive review. Energy Convers Manag 2023;286:117035. https://doi.org/10.1016/J.ENCONMAN.2023.117035.
[2] G.P. Thiel, D.E.M. Warsinger, L.D. Banchik, J.H. Lienhard, Low Carbon Desalination: Status and Research, Development, and Demonstration Needs, Report of a workshop conducted at the Massachusetts Institute of Technology in association with the Global Clean Water Desalination Alliance, Prof. Lienhard via Angie Locknar (2016). https://dspace.mit.edu/handle/1721.1/105755 (accessed January 24, 2024).
[3] Global Clean Water Desalination Alliance "H 2 0 minus CO 2 ", (n.d.).
[4] Aboelmaaref MM, Zayed ME, Zhao J, Li W, Askalany AA, Salem Ahmed M, et al. Hybrid solar desalination systems driven by parabolic trough and parabolic dish CSP technologies: technology categorization, thermodynamic performance and economical assessment. Energy Convers Manag 2020;220:113103. https://doi.org/10.1016/j.enconman.2020.113103.
[5] Ghaffour N, Lattemann S, Missimer T, Ng KC, Sinha S, Amy G. Renewable energy-driven innovative energy-efficient desalination technologies. Appl Energy 2014;136:1155–65. https://doi.org/10.1016/j.apenergy.2014.03.033.

[6] Ghazi ZM, Rizvi SWF, Shahid WM, Abdulhameed AM, Saleem H, Zaidi SJ. An overview of water desalination systems integrated with renewable energy sources. Desalination 2022;542:116063. https://doi.org/10.1016/J.DESAL.2022.116063.

[7] European Climate Law, (n.d.). https://ec.europa.eu/clima/eu-action/european-green-deal/european-climate-law_en (accessed August 3, 2022).

[8] Ali A, Tufa RA, Macedonio F, Curcio E, Drioli E. Membrane technology in renewable-energy-driven desalination. Renew Sustain Energy Rev 2018;81:1–21. https://doi.org/10.1016/J.RSER.2017.07.047.

[9] Okampo EJ, Nwulu N. Optimisation of renewable energy powered reverse osmosis desalination systems: a state-of-the-art review. Renew Sustain Energy Rev 2021; 140:110712. https://doi.org/10.1016/J.RSER.2021.110712.

[10] Yilmaz F. Design and performance analysis of hydro and wind-based power and hydrogen generation system for sustainable development. Sustainable Energy Technol Assess 2024;64:103742. https://doi.org/10.1016/J.SETA.2024.103742.

[11] Cherif H, Belhadj J. Environmental life cycle analysis of water desalination processes, sustainable desalination handbook: plant selection. Design Implement 2018:527–59. https://doi.org/10.1016/B978-0-12-809240-8.00015-0.

[12] Abdelkareem MA, El Haj Assad M, Sayed ET, Soudan B. Recent progress in the use of renewable energy sources to power water desalination plants. Desalination 2018;435:97–113.

[13] Kucera J. Introduction to desalination. Desalination 2019:1–49. https://doi.org/10.1002/9781119407874.CH1.

[14] J. González, P. Cabrera, J.A. Carta, Wind Energy Powered Desalination Systems, in: Desalination, Wiley; 2019: pp. 567–646. Doi: 10.1002/9781119407874.ch14.

[15] Gómez-Gotor A, Del Río-Gamero B, Prieto Prado I, Casañas A. The history of desalination in the Canary Islands. Desalination 2018;428:86–107.

[16] C. Matos, P. Cabrera, J.A. Carta, N. Melián-Martel, Wind-powered desalination on islands: a review of energy–water pathways, J Mar Sci Eng 2024, Vol. 12, p. 464 12 (2024) 464. Doi: 10.3390/JMSE12030464.

[17] Cabrera P, Carta JA, Matos C, Rosales-Asensio E, Lund H. Reduced desalination carbon footprint on islands with weak electricity grids. The Case of Gran Canaria, Appl Energy 2024;358:122564. https://doi.org/10.1016/J.APENERGY.2023.122564.

[18] Gude VG. Energy storage for desalination processes powered by renewable energy and waste heat sources. Appl Energy 2015;137:877–98. https://doi.org/10.1016/J.APENERGY.2014.06.061.

[19] Carta JA, González J. Self-sufficient energy supply for isolated communities: Wind-diesel systems in the Canary Islands. Energy J 2001;22:115–45. https://doi.org/10.5547/issn0195-6574-ej-vol22-no3-5.

[20] Carta JA, González J, Gómez C. Operating results of a wind–diesel system which supplies the full energy needs of an isolated village community in the Canary Islands. Sol Energy 2003;74:53–63. https://doi.org/10.1016/S0038-092X(03)00108-7.

[21] Cabrera P, Carta JA, González J, Melián G. Wind-driven SWRO desalination prototype with and without batteries: a performance simulation using machine learning models. Desalination 2018;435:77–96. https://doi.org/10.1016/J.DESAL.2017.11.044.

[22] Carta JA, Cabrera P. Optimal sizing of stand-alone wind-powered seawater reverse osmosis plants without use of massive energy storage. Appl Energy 2021;304: 117888. https://doi.org/10.1016/J.APENERGY.2021.117888.

[23] Carta JA, González J, Subiela V. Operational analysis of an innovative wind powered reverse osmosis system installed in the Canary Islands. Sol Energy 2003; 75. https://doi.org/10.1016/S0038-092X(03)00247-0.

[24] Carta JA, González J, Subiela V. The SDAWES project: an ambitious R&D prototype for wind-powered desalination. Desalination 2004;161:33–48. https://doi.org/10.1016/S0011-9164(04)90038-0.

[25] Carta JA, González J, Cabrera P, Subiela VJ. Preliminary experimental analysis of a small-scale prototype SWRO desalination plant, designed for continuous adjustment of its energy consumption to the widely varying power generated by a stand-alone wind turbine. Appl Energy 2015;137:222–39. https://doi.org/10.1016/J.APENERGY.2014.09.093.

[26] Sohrabi A, Meratizaman M, Liu S. Comparative analysis of integrating standalone renewable energy sources with brackish water reverse osmosis plants: Technical and economic perspectives. Desalination 2024;571:117106. https://doi.org/10.1016/J.DESAL.2023.117106.

[27] Cabrera P, Carta JA, Matos C, Lund H. Lessons learned in wind-driven desalination systems in the Canary Islands: useful knowledge for other world islands. Desalination 2024;583:117697. https://doi.org/10.1016/J.DESAL.2024.117697.

[28] Lai W, Ma Q, Lu H, Weng S, Fan J, Fang H. Effects of wind intermittence and fluctuation on reverse osmosis desalination process and solution strategies. Desalination 2016;395:17–27. https://doi.org/10.1016/J.DESAL.2016.05.019.

[29] Lising ER, Alward R. Unsteady state operation of a reverse osmosis desalination unit. Desalination 1972;11:261–8. https://doi.org/10.1016/S0011-9164(00)80132-0.

[30] The application of wind energy systems to desalination (Technical Report) | OSTI. GOV, (n.d.). https://www.osti.gov/biblio/7012329 (accessed January 29, 2024).

[31] Petersen G, Fries S, Mohn J, Müller A. Wind and solar powered reverse osmosis desalination units - design, start up, operating experience. Desalination 1981;39: 125–35. https://doi.org/10.1016/S0011-9164(00)86115-9.

[32] McBride R, Morris R, Hanbury W. Wind power a reliable source for desalination. Desalination 1987;67:559–64. https://doi.org/10.1016/0011-9164(87)90269-4.

[33] Petersen G, Fries S, Mohn J, Müller A. Wind and solar-powered reverse osmosis desalination units - description of two demonstration projects-. Desalination 1979; 31:501–9. https://doi.org/10.1016/S0011-9164(00)88553-7.

[34] Maurel A. Dessalement et energies nouvelles. Desalination 1979;31:489–99. https://doi.org/10.1016/S0011-9164(00)88552-5.

[35] Libert JJ, Maurel A. Desalination and renewable energies-a few recent developments. Desalination 1981;39:363–72. https://doi.org/10.1016/S0011-9164(00)86141-X.

[36] The Life of a Reverse Osmosis Membrane, Part 1 | Pumps & Systems, (n.d.). https://www.pumpsandsystems.com/life-reverse-osmosis-membrane-part-1 (accessed February 10, 2024).

[37] Desalination Engineering: Planning and Design, (n.d.). https://www.mhprofessional.com/desalination-engineering-planning-and-design-9780071777155-usa (accessed February 10, 2024).

[38] Jiang S, Li Y, Ladewig BP. A review of reverse osmosis membrane fouling and control strategies. Sci Total Environ 2017;595:567–83. https://doi.org/10.1016/J.SCITOTENV.2017.03.235.

[39] Park GL, Schäfer AI, Richards BS. The effect of intermittent operation on a wind-powered membrane system for brackish water desalination. Water Sci Technol 2012;65:867–74. https://doi.org/10.2166/WST.2012.912.

[40] M. Freire-Gormaly, A. Bilton, An experimental system for characterization of membrane fouling of solar photovoltaic reverse osmosis systems under intermittent operation, (2017) 22–26. Doi: 10.5004/dwt.2017.20391.

[41] Freire-Gormaly M, Bilton AM. Experimental quantification of the effect of intermittent operation on membrane performance of solar powered reverse osmosis desalination systems. Desalination 2018;435:188–97. https://doi.org/10.1016/J.DESAL.2017.09.013.

[42] Sarker NR, Bilton AM. Real-time computational imaging of reverse osmosis membrane scaling under intermittent operation. J Memb Sci 2021;636:119556. https://doi.org/10.1016/J.MEMSCI.2021.119556.

[43] Kim HW, Choi W, Suh D, Baek Y, Cho K, Jeong S. Pilot study of biofouling occurrence in a brackish water reverse osmosis system using intermittent operation. J Clean Prod 2023;425:139097. https://doi.org/10.1016/J.JCLEPRO.2023.139097.

[44] S. Lee, H. Cho, Y. Choi, S. Lee, Application of Optical Coherence Tomography (OCT) to Analyze Membrane Fouling under Intermittent Operation, Membranes 2023, Vol. 13, P. 392 13 (2023) 392. Doi: 10.3390/MEMBRANES13040392.

[45] Yang H, Choi J, Choi Y, Lee S. Effect of intermittent operation modes on performance of reverse osmosis (RO) membrane in desalination and water treatment. Membr Water Treat 2022;13:39–49. https://doi.org/10.12989/MWT.2022.13.1.039.

[46] Ruiz-García A, Nuez I. Long-term intermittent operation of a full-scale BWRO desalination plant. Desalination 2020;489:114526. https://doi.org/10.1016/J.DESAL.2020.114526.

[47] Cai Y-H, Boussouga Y-A, Schäfer AI. Renewable energy powered membrane technology: impact of intermittency on membrane integrity. Desalination 2024: 117504. https://doi.org/10.1016/J.DESAL.2024.117504.

[48] Penña N, Gallego S, del Vigo F, Chesters SP. Evaluating impact of fouling on reverse osmosis membranes performance. Desalination Water Treat 2013;51: 958–68. https://doi.org/10.1080/19443994.2012.699509.

[49] A Study Of The Physical And Chemical Damage On Reverse Osmosis Membranes Detected By Autopsies - AquaEnergy Expo Knowledge Hub, (n.d.). https://kh.aquaenergyexpo.com/product/a-study-of-the-physical-and-chemical-damage-on-reverse-osmosis-membranes-detected-by-autopsies/ (accessed March 17, 2024).

[50] Desalplus – Desalplus desalination lab, (n.d.). https://www.desalinationlab.com/ (accessed April 25, 2024).

[51] Vitec™ 3000, Liquid Antiscalant - Avista™, (n.d.). https://avistamembranesolutions.com/products/vitec-3000/ (accessed February 7, 2024).

[52] Salinnova – Salinnova, (n.d.). https://www.salinnova.com/ (accessed February 6, 2024).

[53] Hydranautics RO Membranes - Pure Aqua, Inc., (n.d.). https://pureaqua.com/hydranautics-membranes/ (accessed February 9, 2024).

[54] Element Loading Guidelines, (2013).

[55] Typical Start-Up Sequence (cont.), (2022). www.dupont.com/water/contact-us (accessed February 16, 2024).

[56] D4516 Standard Practice for Standardizing Reverse Osmosis Performance Data, (n.d.). https://www.astm.org/d4516-19a.html (accessed February 9, 2024).

[57] Reverse Osmosis: Design, Processes, and Applications for Engineers | Wiley, (n.d.). https://www.wiley.com/en-gb/Reverse+Osmosis:+Design,+Processes,+and+Applications+for+Engineers-p-9780470882634 (accessed February 20, 2024).

[58] T.A. Membrane Europe, Operation, Maintenance and Handling Manual for membrane elements Lenntech, (n.d.). www.lenntech.comFax. (accessed February 20, 2024).

[59] Technical Service Bulletins (TSB) | Technical Bulletins | LG Water Solutions, (n.d.). https://www.lgwatersolutions.com/en/technical-document/technical-bulletins-tsb (accessed February 20, 2024).

[60] What Is Membrane Performance Normalization? - PDF Free Download, (n.d.). https://docplayer.net/21032491-What-is-membrane-performance-normalization.html (accessed February 20, 2024).

[61] FilmTec™ Reverse Osmosis Membranes Technical Manual; 2023.

[62] Farhat S, Bali M, Kamel F. Membrane autopsy to provide solutions to operational problems of Jerba brackish water desalination plant. Desalination 2018;445: 225–35. https://doi.org/10.1016/J.DESAL.2018.08.013.

[63] Jane. Kucera, Reverse osmosis : design, processes, and applications for engineers, (2010) 393. https://www.wiley.com/en-gb/Reverse+Osmosis%3A+Design%2C+Processes%2C+and+Applications+for+Engineers-p-9780470882634 (accessed February 20, 2024).

[64] randomForest: Breiman and Cutler's Random Forests for Classification and Regression | Enhanced Reader, (n.d.). moz-extension://98eb39f8-558b-43a0-8f29-c82d0d903c14/enhanced-reader.html?openApp&pdf=https%3A%2F%2Fcran.r-

project.org%2Fweb%2Fpackages%2FrandomForest%2FrandomForest.pdf (accessed February 20, 2023).
[65] Díaz S, Carta JA, Matías JM. Performance assessment of five MCP models proposed for the estimation of long-term wind turbine power outputs at a target site using three machine learning techniques. Appl Energy 2018;209:455–77. https://doi.org/10.1016/J.APENERGY.2017.11.007.
[66] randomForest: Breiman and Cutler's random forests for classification and regression version 4.6-10 from R-Forge, (n.d.). https://rdrr.io/rforge/randomForest/ (accessed February 20, 2023).
[67] R: The R Project for Statistical Computing, (n.d.). https://www.r-project.org/ (accessed February 20, 2023).
[68] Breiman L. Random forests. Mach Learn 2001;45:5–32. https://doi.org/10.1023/A:1010933404324.
[69] Díaz S, Carta JA, Matías JM. Comparison of several measure-correlate-predict models using support vector regression techniques to estimate wind power densities. A Case Study, Energy Convers Manag 2017;140:334–54. https://doi.org/10.1016/J.ENCONMAN.2017.02.064.
[70] Ross SM. Introduction to Probability and Statistics for Engineers and Scientists. Sixth Edition, Sixth, Elsevier 2020. https://doi.org/10.1016/C2018-0-02166-0.
[71] Shapiro SS, Wilk MB. An Analysis of Variance Test for Normality (Complete Samples). Biometrika 1965;52:591. https://doi.org/10.2307/2333709.
[72] Kalpić D, Hlupić N, Lovrić M. Student's t-Tests, International Encyclopedia of. Stat Sci 2011:1559–63. https://doi.org/10.1007/978-3-642-04898-2_641.
[73] R.R. Wilcox, Introduction to Robust Estimation and Hypothesis Testing: 4th Edition, Introduction to Robust Estimation and Hypothesis Testing: 4th Edition (2016) 1–786.
[74] Ellis PD. The essential guide to effect sizes: statistical power, meta-analysis, and the interpretation of research results. Essential Guide Effect Siz 2010. https://doi.org/10.1017/CBO9780511761676.
[75] R.J. Grissom, J.J. Kim, Effect sizes for research: Univariate and multivariate applications, second edition, Effect Sizes for Research: Univariate and Multivariate Applications, Second Edition (2012) 1–434. Doi: 10.4324/9780203803233/EFFECT-SIZES-RESEARCH-ROBERT-GRISSOM-JOHN-KIM.
[76] J. Cohen, Statistical power for the behaviour sciences, 1977. http://www.sciencedirect.com:5070/book/9780121790608/statistical-power-analysis-for-the-behavioral-sciences (accessed April 6, 2024).
[77] T. Hastie, R. Tibshirani, J. Friedman, The Elements of Statistical Learning, 2009. Doi: 10.1007/978-0-387-84858-7.
[78] Reverse Osmosis Normalization | Reverse Osmosis | Puretec Industrial Water, (n.d.). https://puretecwater.com/reverse-osmosis/reverse-osmosis-normalization (accessed April 8, 2024).